Supplemental file-

Underestimation of historical terrestrial water storage droughts in global water models

Amar Deep Tiwari[1], Yadu Pokhrel[1], Farshid Felfelani[2], Ahmed Elkouk[1], Julien Boulange[3], Simon N. Gosling[4], Naota Hanasaki[5], Aristeidis Koutroulis[6], Vimal Mishra[7], Hannes Müller Schmied[8,9], Yusuke Satoh[10], Sebastian Ostberg[11], Tobias Stacke[12], Jiabo Yin[13]

[1]Department of Civil and Environmental Engineering, Michigan State University, East Lansing, Michigan, USA

[2]Research Applications Laboratory, National Center for Atmospheric Research, Boulder, CO, USA

[3]United graduate school of agricultural science, Tokyo University of Agriculture and Technology, Fuchu, Tokyo, Japan

[4]School of Geography, University of Nottingham, Nottingham, UK

[5]National Institute for Environmental Studies (NIES), Tsukuba, Japan

[6]School of Chemical and Environmental Engineering, Technical University of Crete, Chania, Greece

[7]Department of Civil Engineering, Indian Institute of Technology, Gandhinagar, Gujarat, India

[8]Institute of Physical Geography, Goethe University Frankfurt, Frankfurt am Main, Germany

[9]Senckenberg Leibniz Biodiversity and Climate Research Centre (SBiK-F), Frankfurt am Main, Germany

[10]Moon Soul Graduate School of Future Strategy, Korea Advanced Institute of Science and Technology (KAIST), Daejeon, Korea

[11]Potsdam Institute for Climate Impact Research (PIK), Member of the Leibniz Association, Potsdam, Germany

[12]Max Planck Institute for Meteorology, Hamburg, Germany

[13]State Key Laboratory of Water Resources Engineering and Management, Wuhan University, Wuhan, China

Corresponding author: Yadu Pokhrel (ypokhrel@msu.edu)

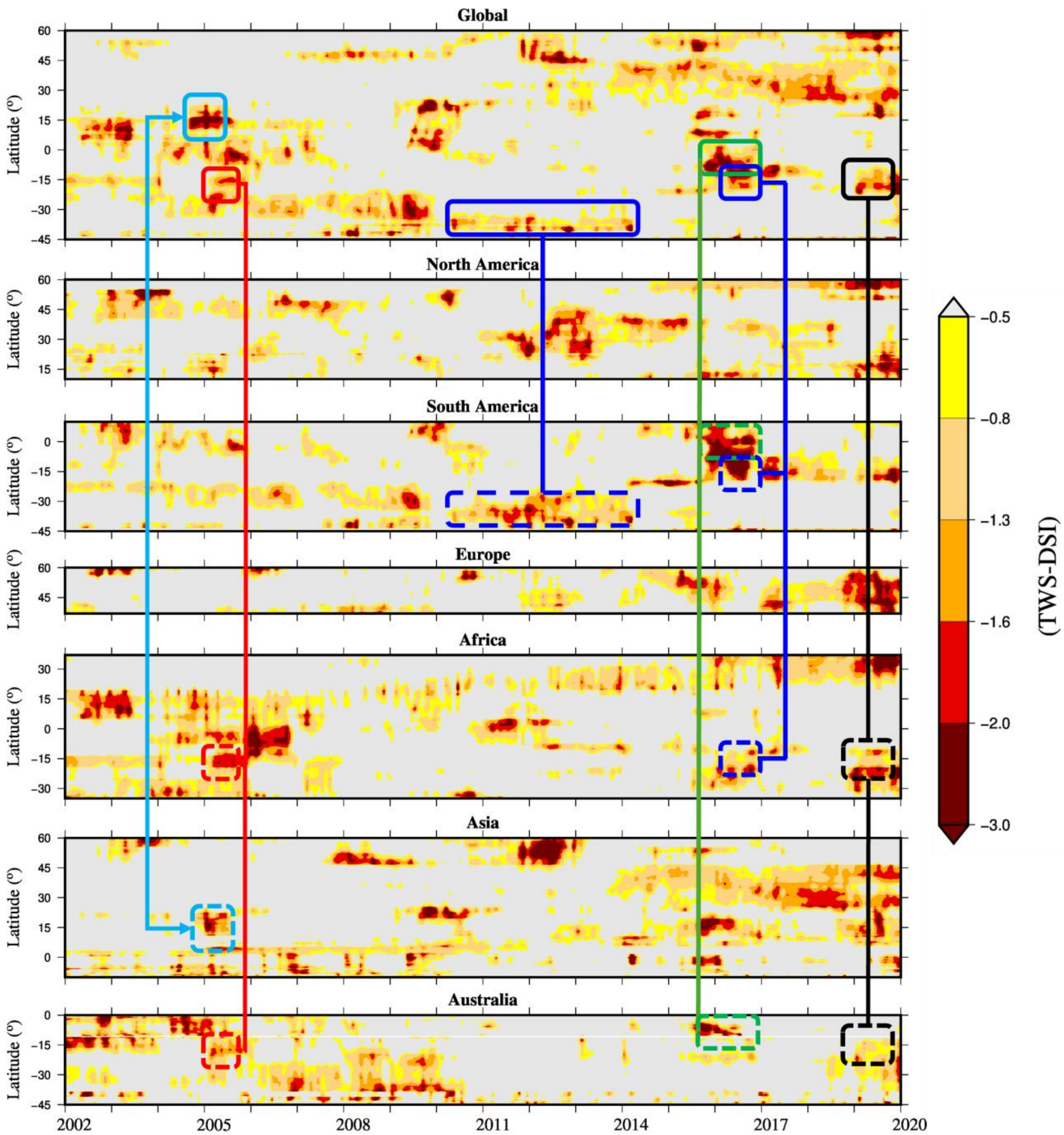

Figure S1: GRACE-based global and corresponding continent-wise TWS droughts in terms of TWS-DSI.

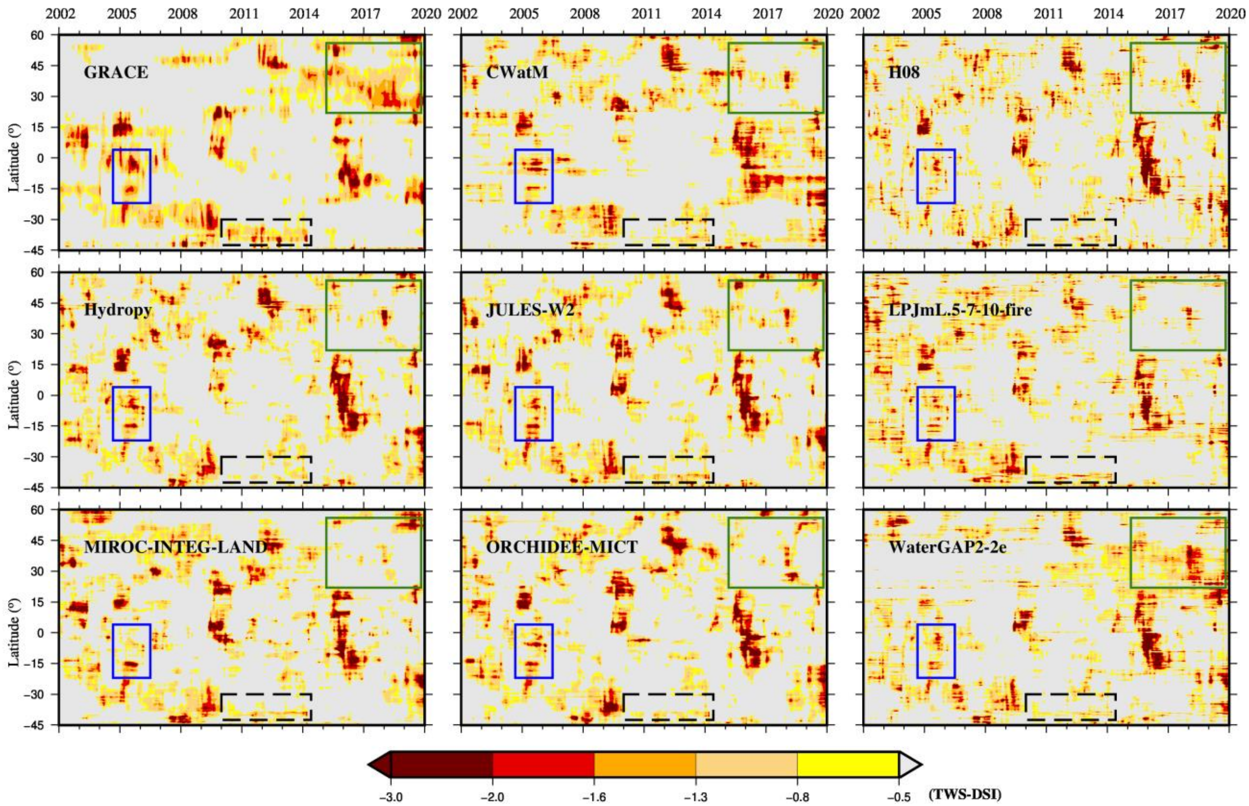

Figure S2. Comparison of individual model TWS droughts against GRACE. Historical TWS latitudinal TWS-DSI from GRACE and the eight individual ISIMIP models are shown here. TWS-DSI are calculated without removing trends from the TWS data.

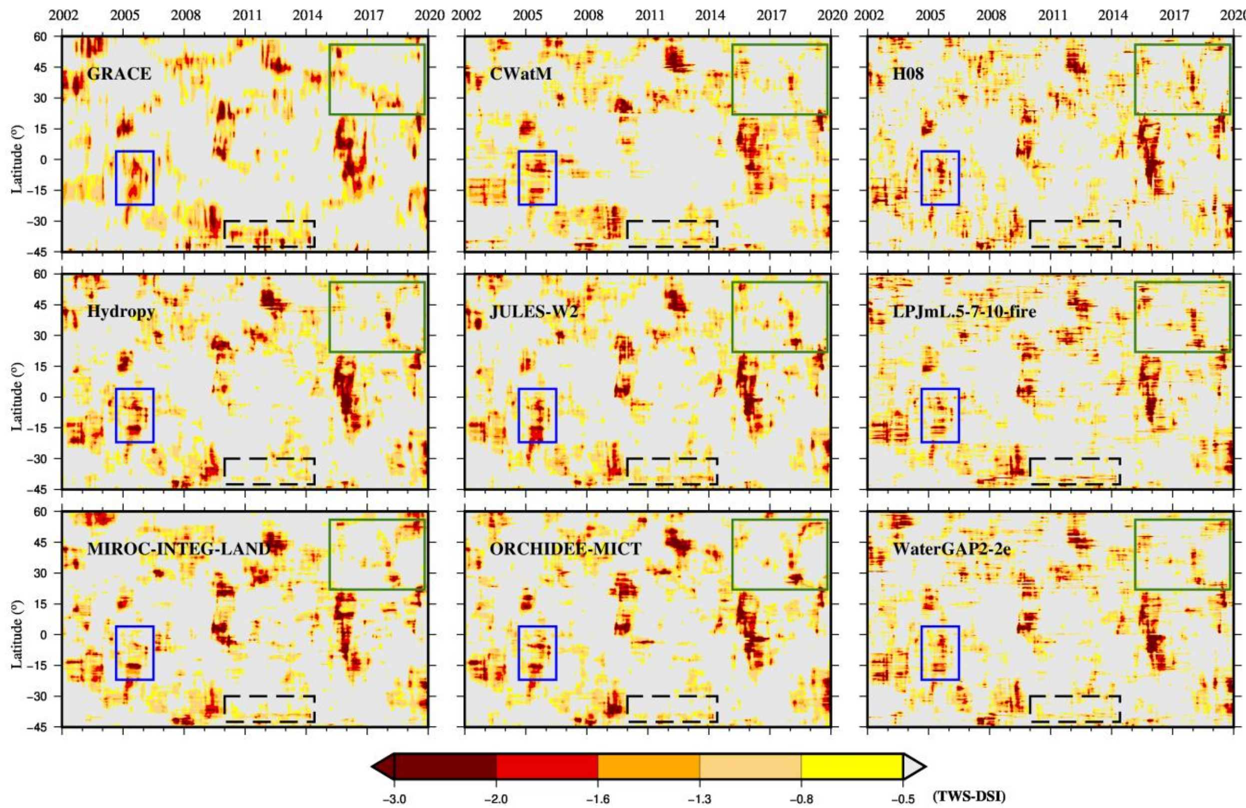

Figure S3. Comparison of individual model TWS droughts against GRACE after removing the linear trends in TWS data.

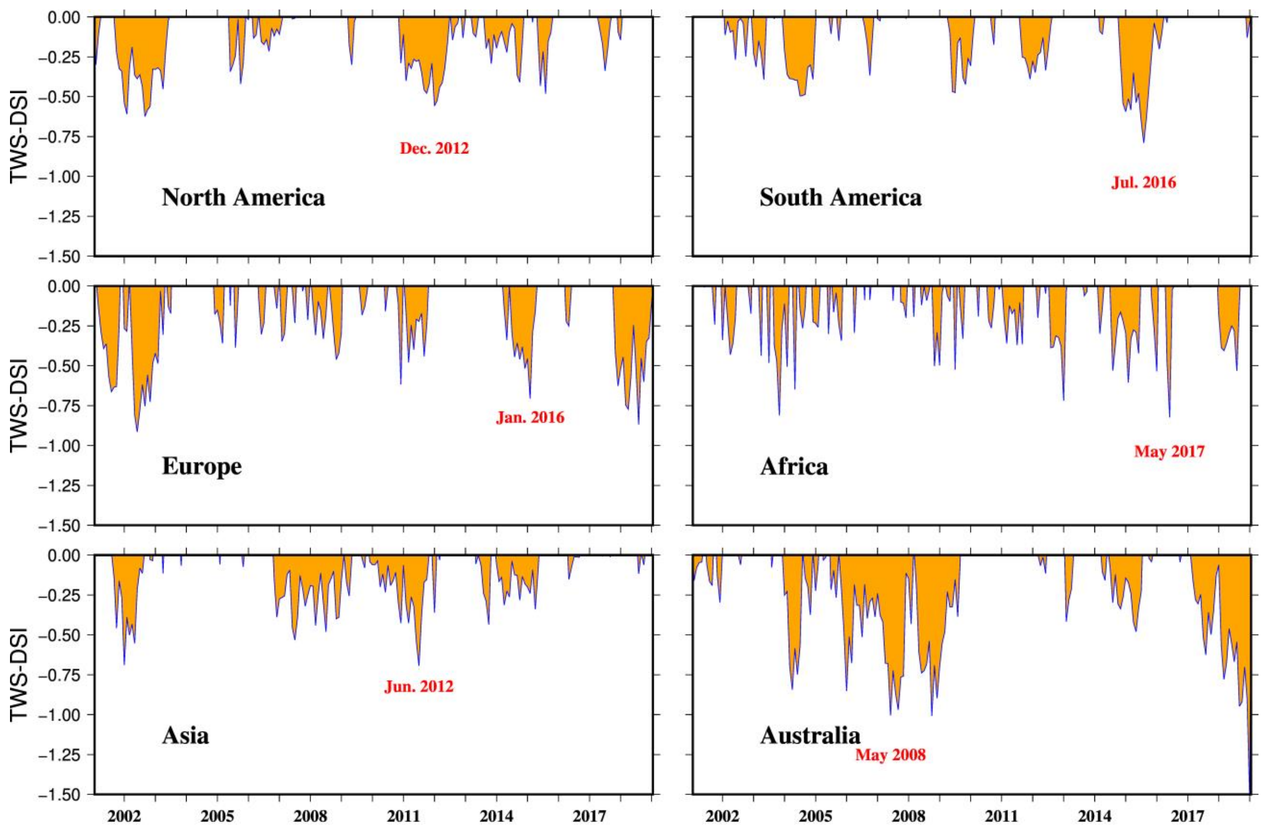

Figure S4. Continent-wise TWS droughts (TWS-DSI) time-series using GRACE.

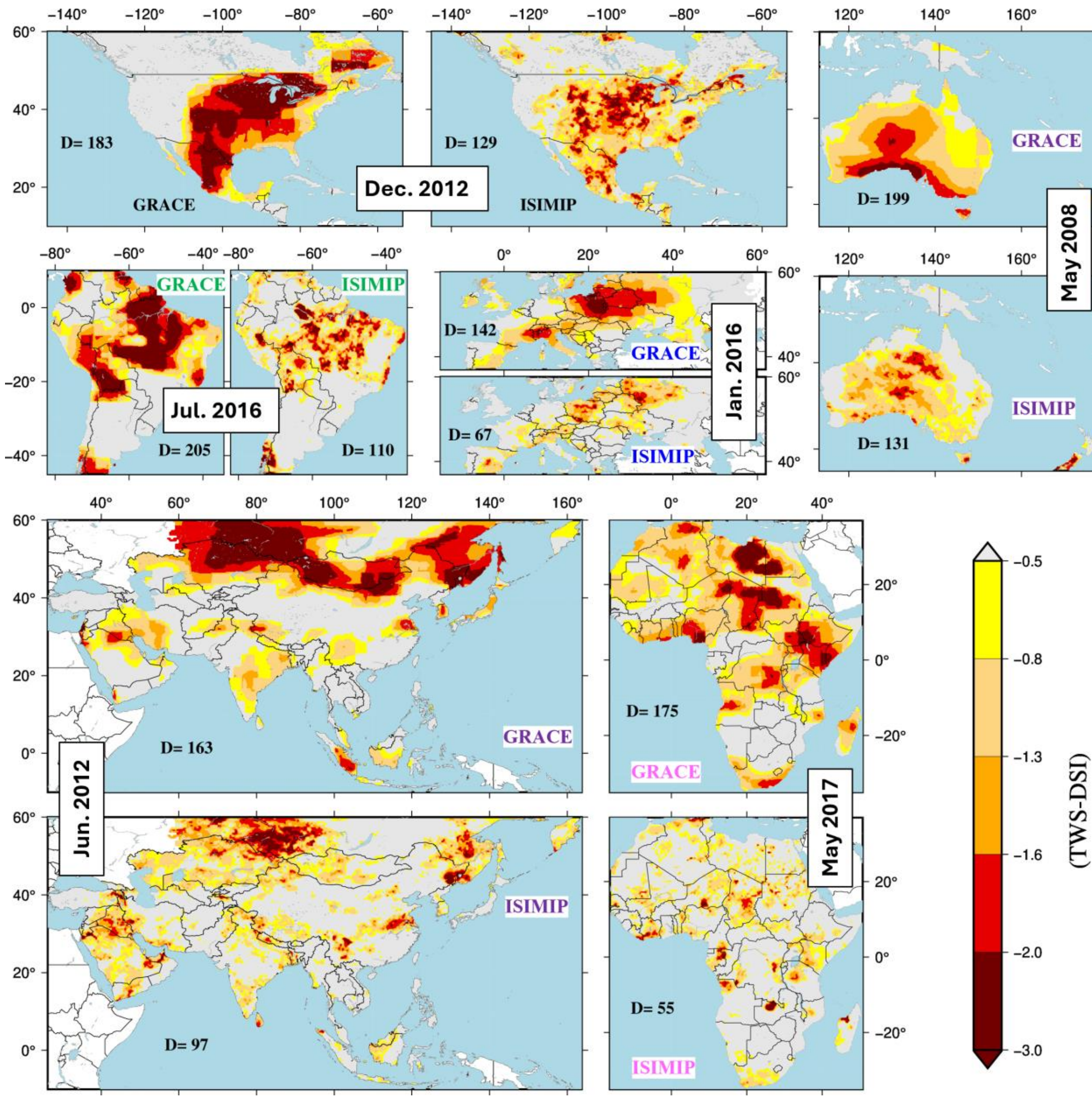

Figure S5. Peak drought comparison using GRACE and model TWS-DSI for continents, North America, South America, Europe, Australia, Asia, and Africa. Here D is DSCI.

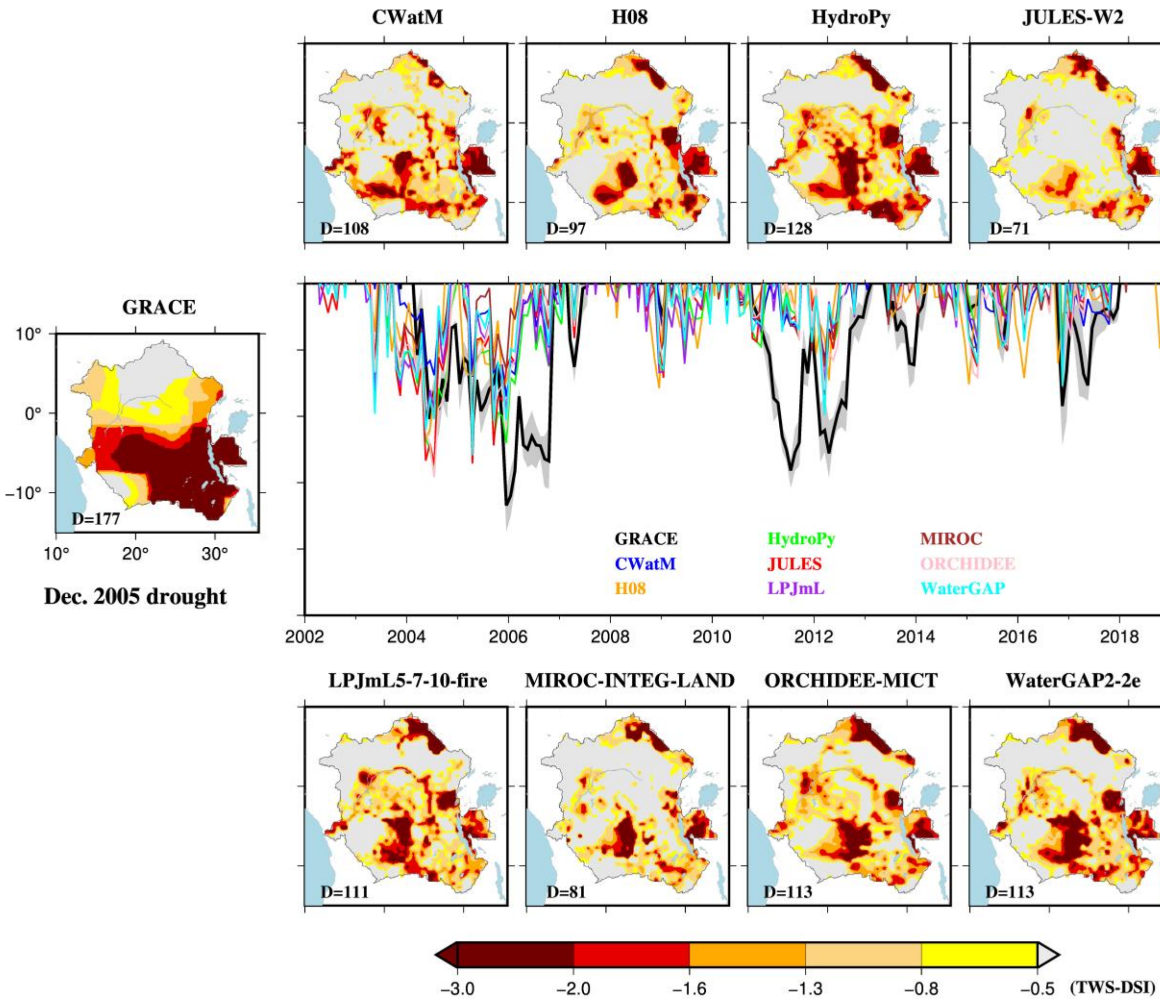

Figure S6. Comparison between GRACE-based and individual model-derived TWS drought with the time series (2002-2019) and spatial distribution of TWS-DSI across the Congo River basin during the peak drought period of December 2005. Grey shaded area shows uncertainty in GRACE data. D values show DSCI.

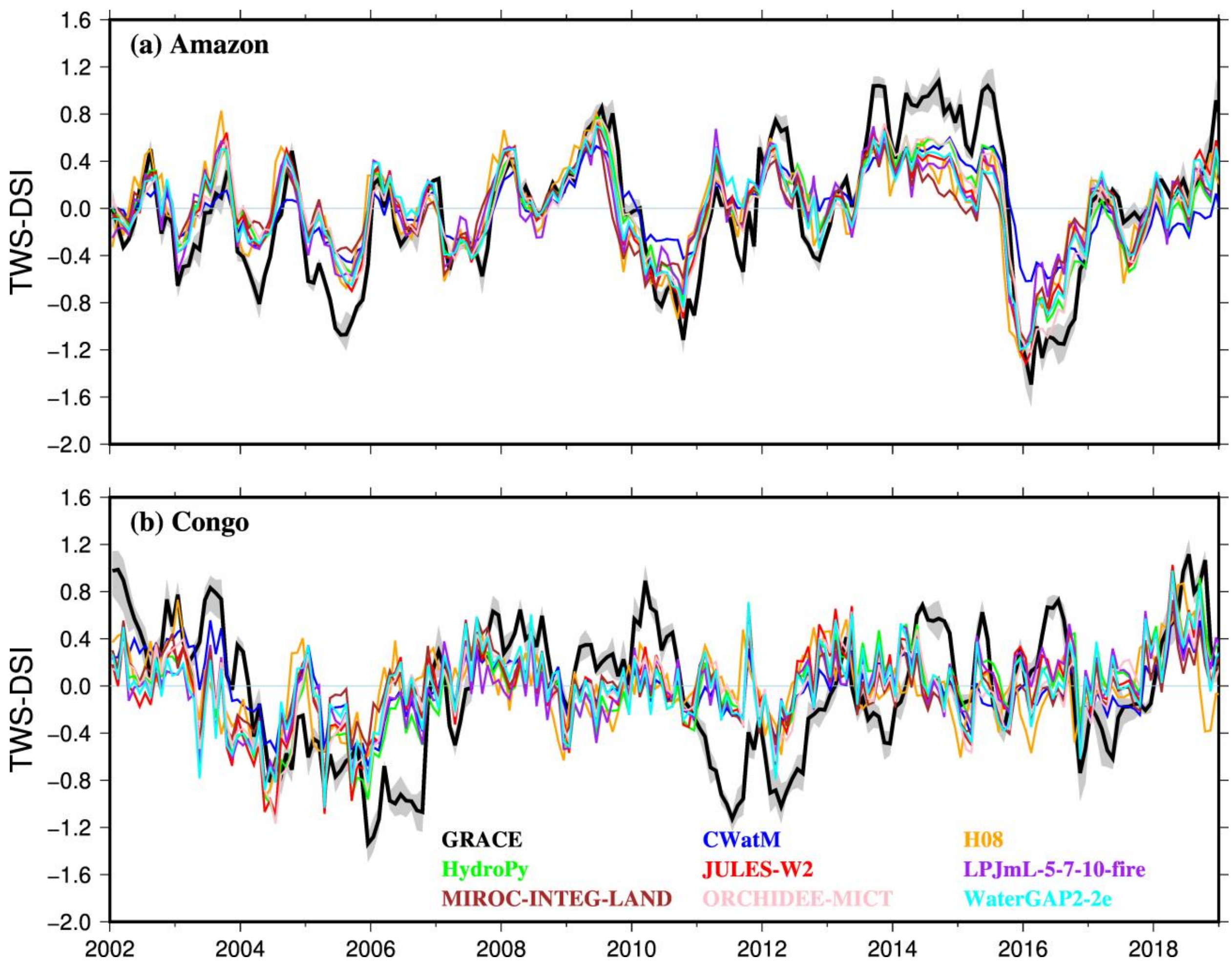

Figure S7: Comparison between GRACE-based and individual model-derived TWS drought with the time series (2002-2019) for (a) Amazon and (b) Congo River basins.

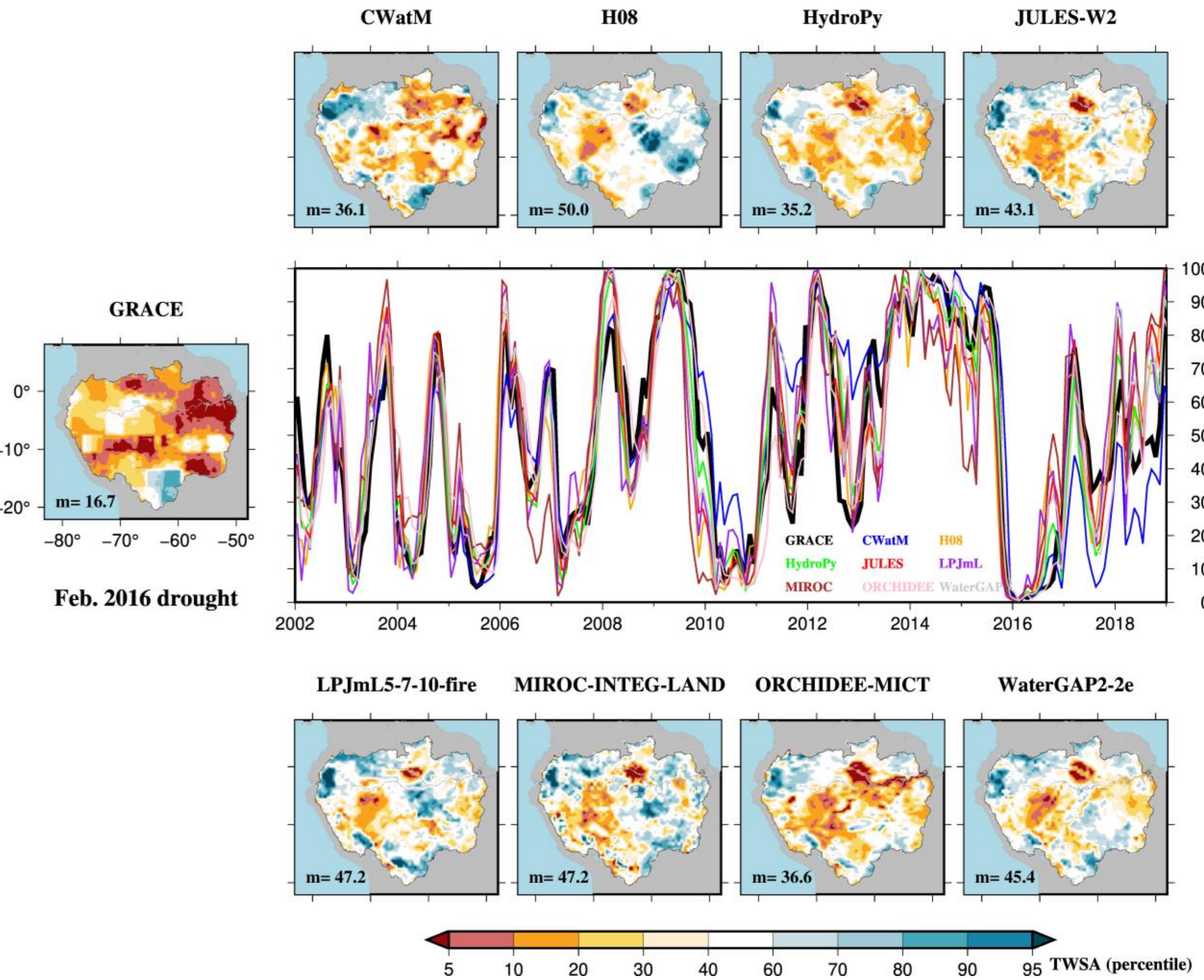

Figure S8. TWSA percentiles comparison using individual model against GRACE for the Amazon River basin. m value shows the basin median.

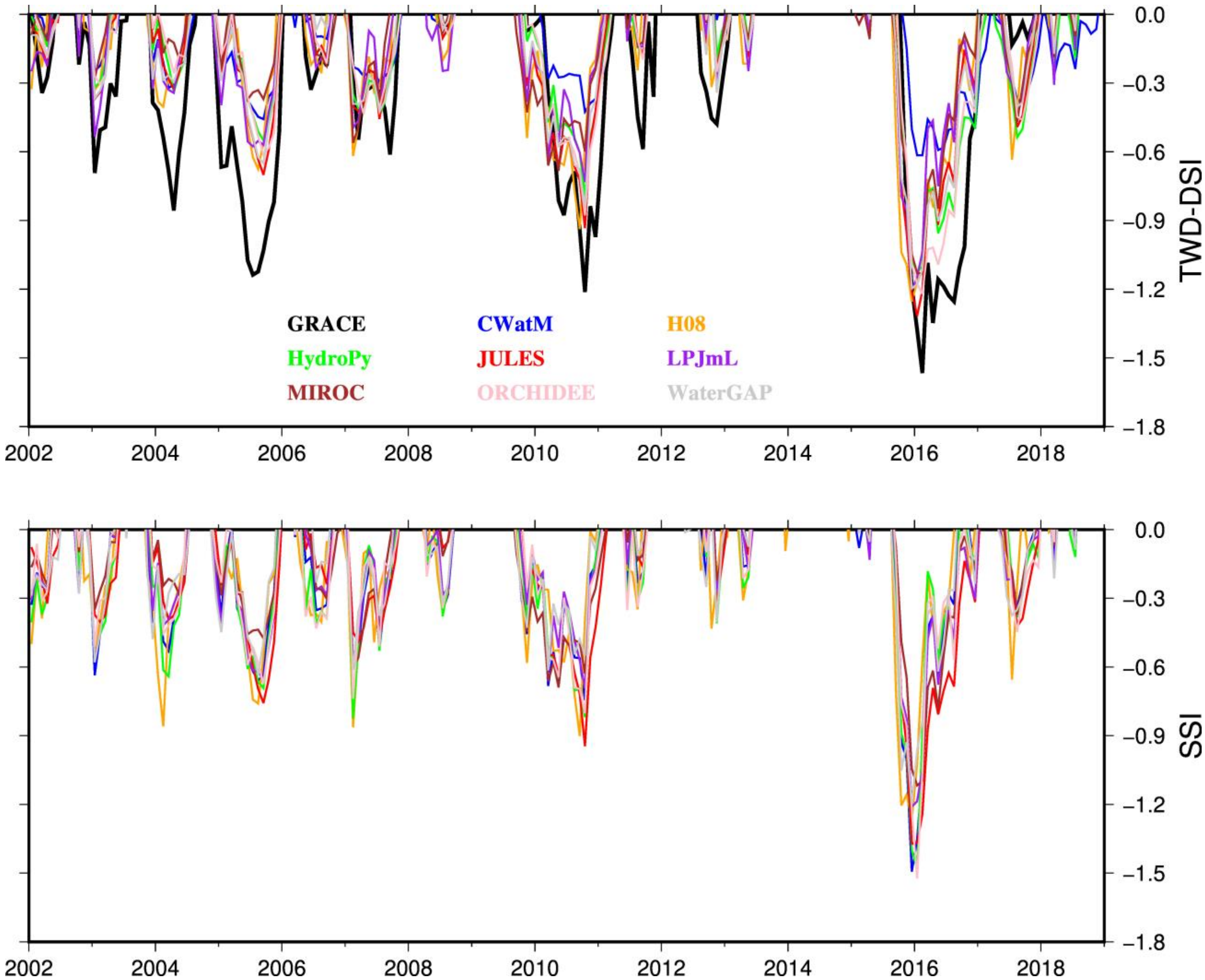

Figure S9. Comparison of TWS-DSI and standardized soil moisture index (SSI) for Amazon River basin.

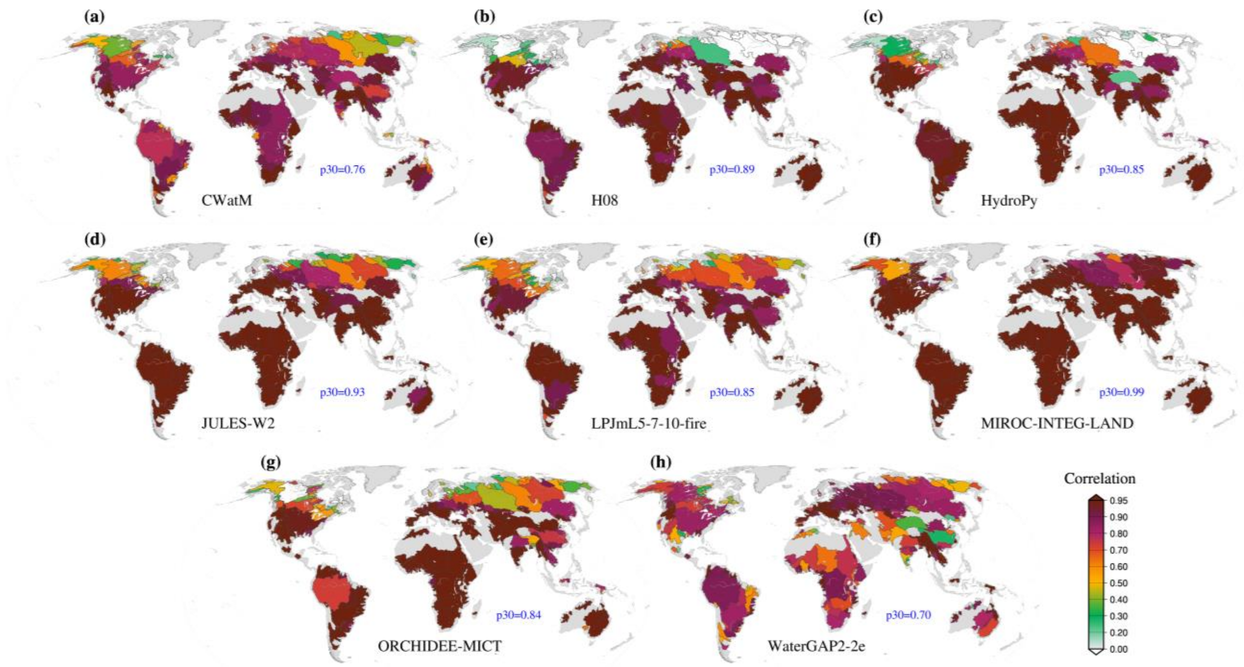

Figure S10. Correlation between basin average model TWS and soil moisture. p30 shows the 30th percentile of correlation of 230 basins.

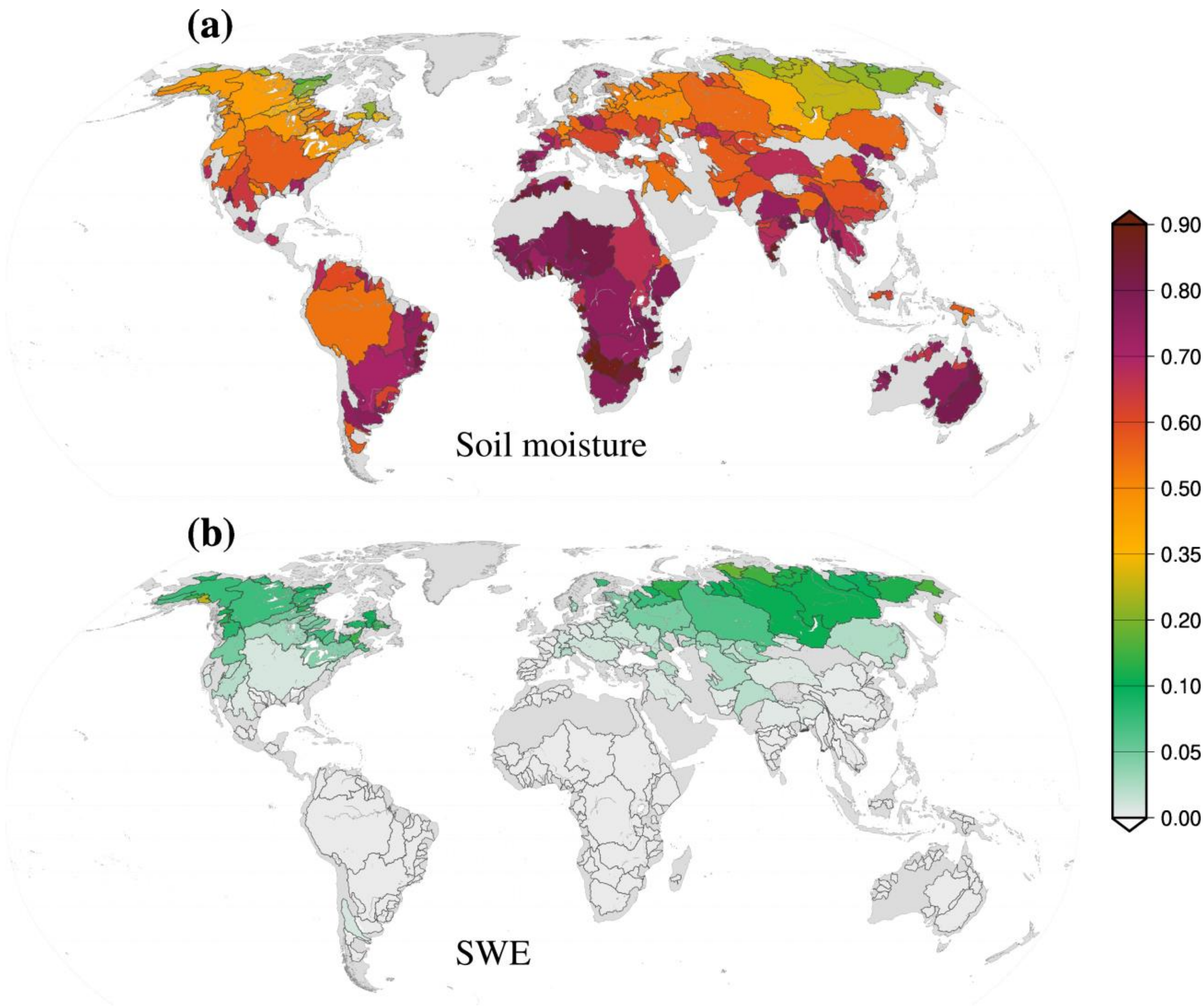

Figure S11. (a) Soil moisture and (b) snow water equivalent (SWE) component contribution ratio (CCR). CCR is the ratio of amplitude of soil moisture or SWE to that of TWS.

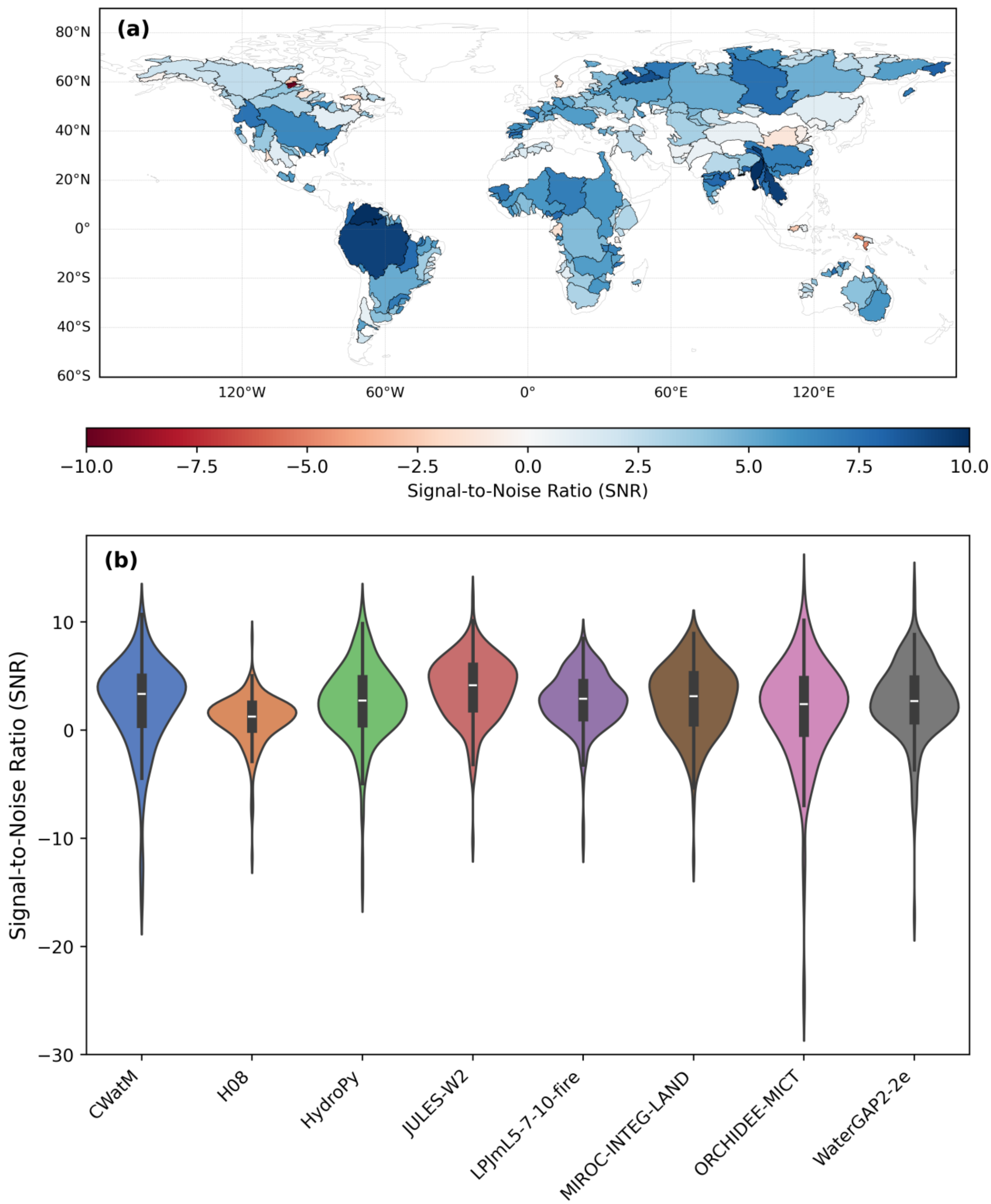

Figure S12. (a) Basin-wise Signal-to-Noise Ratio (SNR) between GRACE TWS and ensemble model TWS, and (b) violin plot showing the SNR distribution for large river basins across eight individual models against observations.

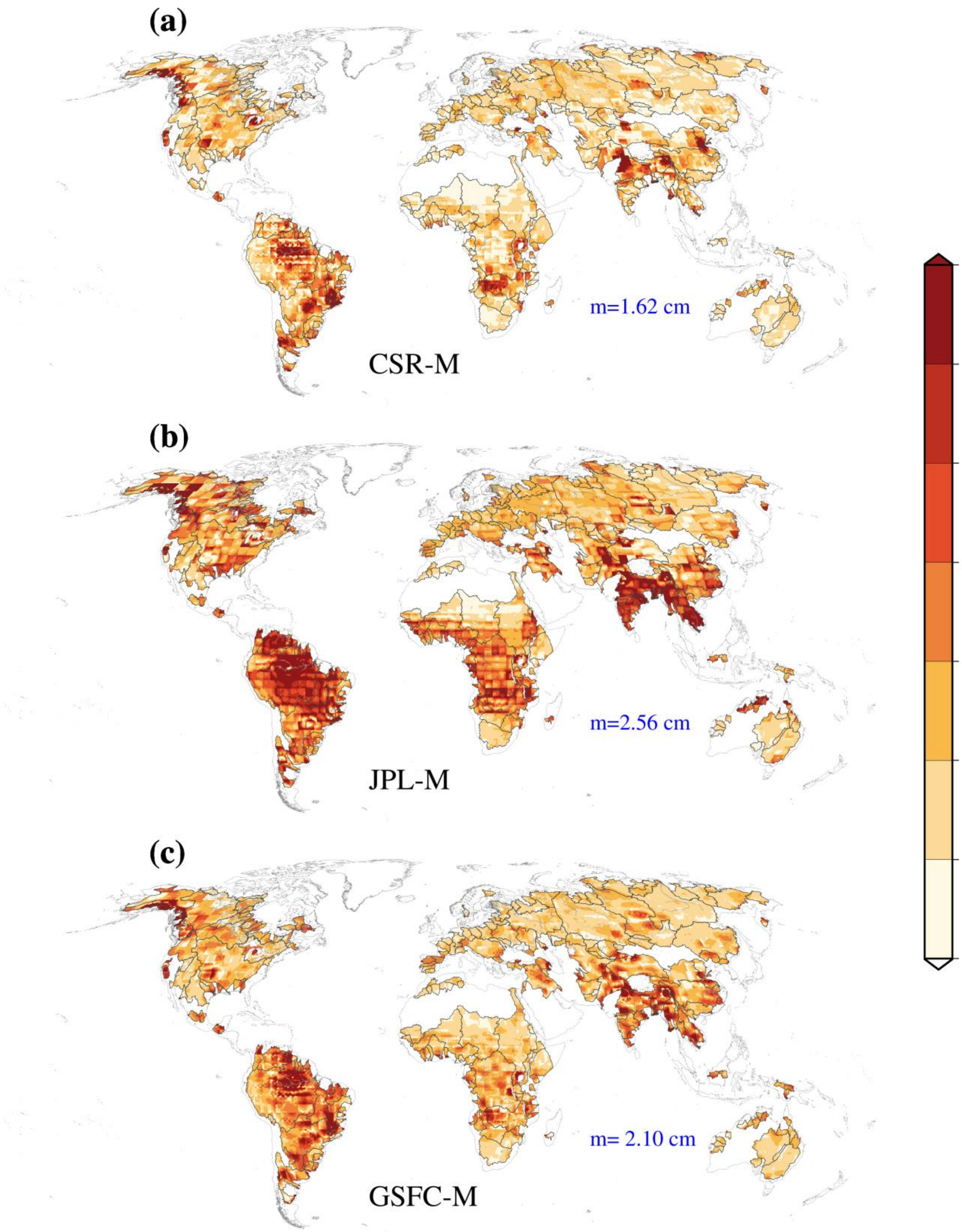
(a)
m=1.62 cm
CSR-M
(b)
m=2.56 cm
JPL-M
(c)
m= 2.10 cm
GSFC-M
7
6
5
4
3
2
1
0

Figure S13. Uncertainties in TWS anomalies for (a) CSR, (b) JPL, and (c) GSFC GRACE mascon products. m values show spatial median.

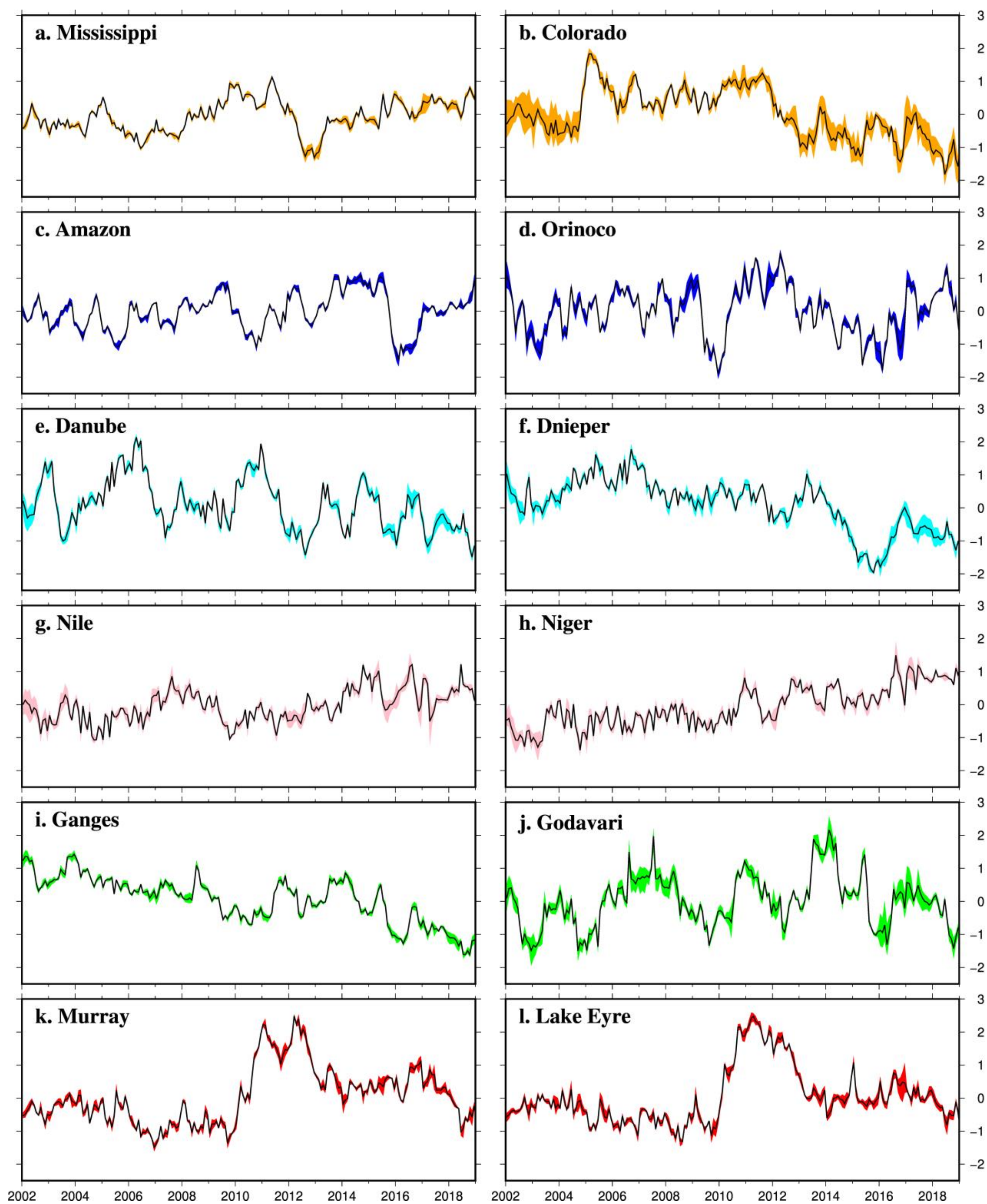

Figure S14. TWS-DSI time-series for 12 river basins, two river basins from each continent, one big and one relatively smaller river. Shaded areas show the maximum and minimum values of TWS anomalies from 3 GRACE products. Black line shows mean of the 3 GRACE products.

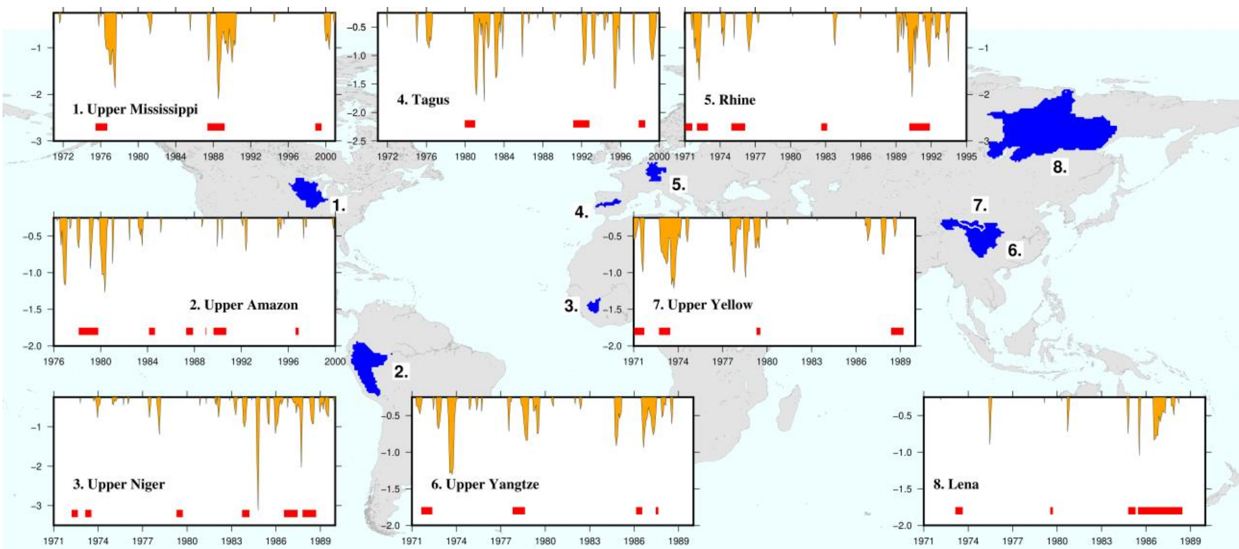

Figure S15. Comparison of observed runoff-based droughts (SRI<-1, identified by Kumar et al., 2024, shown in red lines) with TWS droughts (using GTWS-MLrec data, shown in orange color) for the period of 1971-2000 for climatically diverse River basins. Here the red dashed lines only show temporal coverage of the droughts. The GRDC based discharge datasets have been used by Kumar et al. (2022) to calculate SRI. Basins were also identified by Kumar et al. (2022).

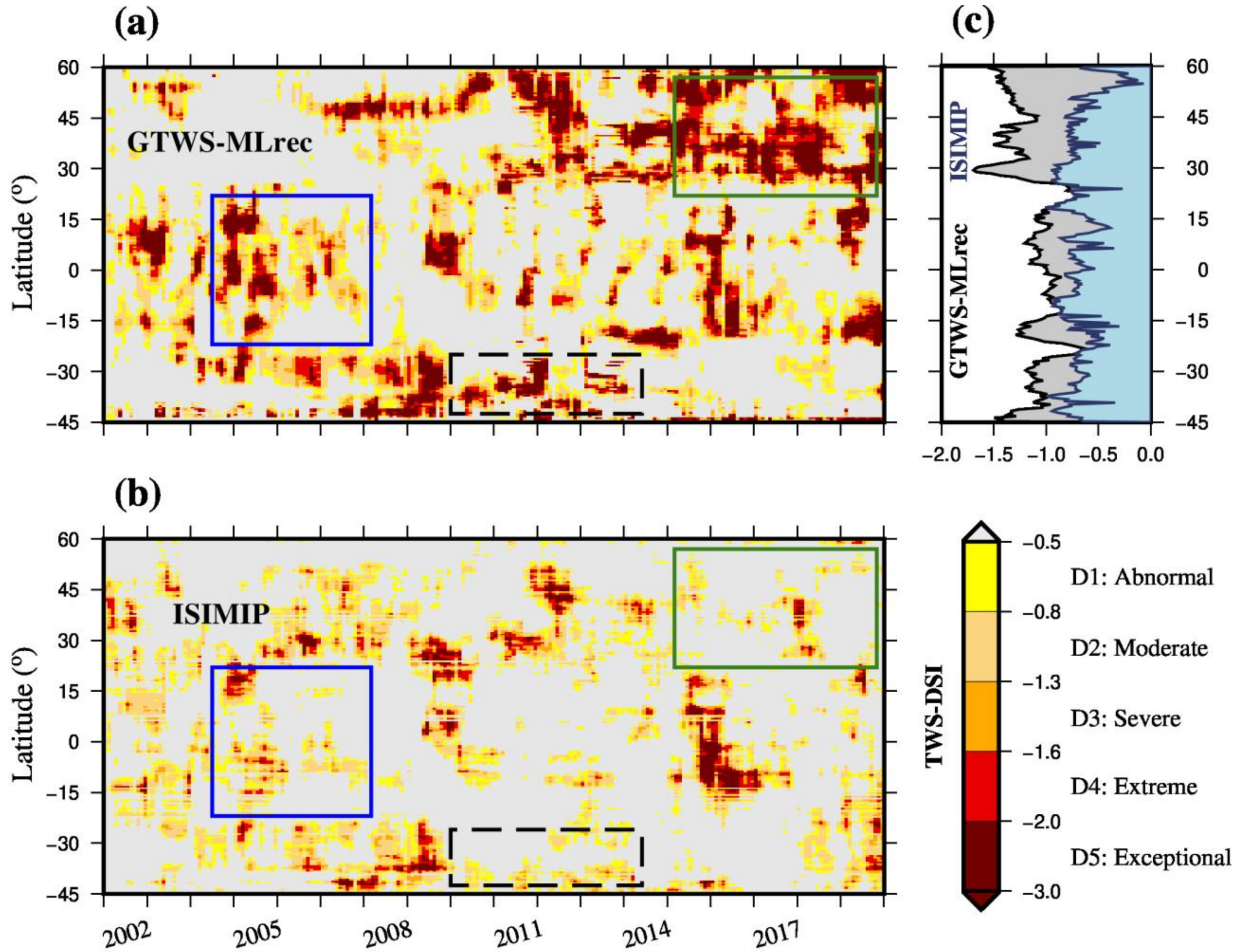

Figure S16. Historical TWS latitudinal droughts from (a) GTWS-MLrec, (b) the ensemble median of eight ISIMIP models, and (c) a comparison of long-term latitudinal simulated droughts against GTWS-MLrec. Here the reference period is 1940-2019. Selected rectangles highlight major droughts underestimated in the simulations.

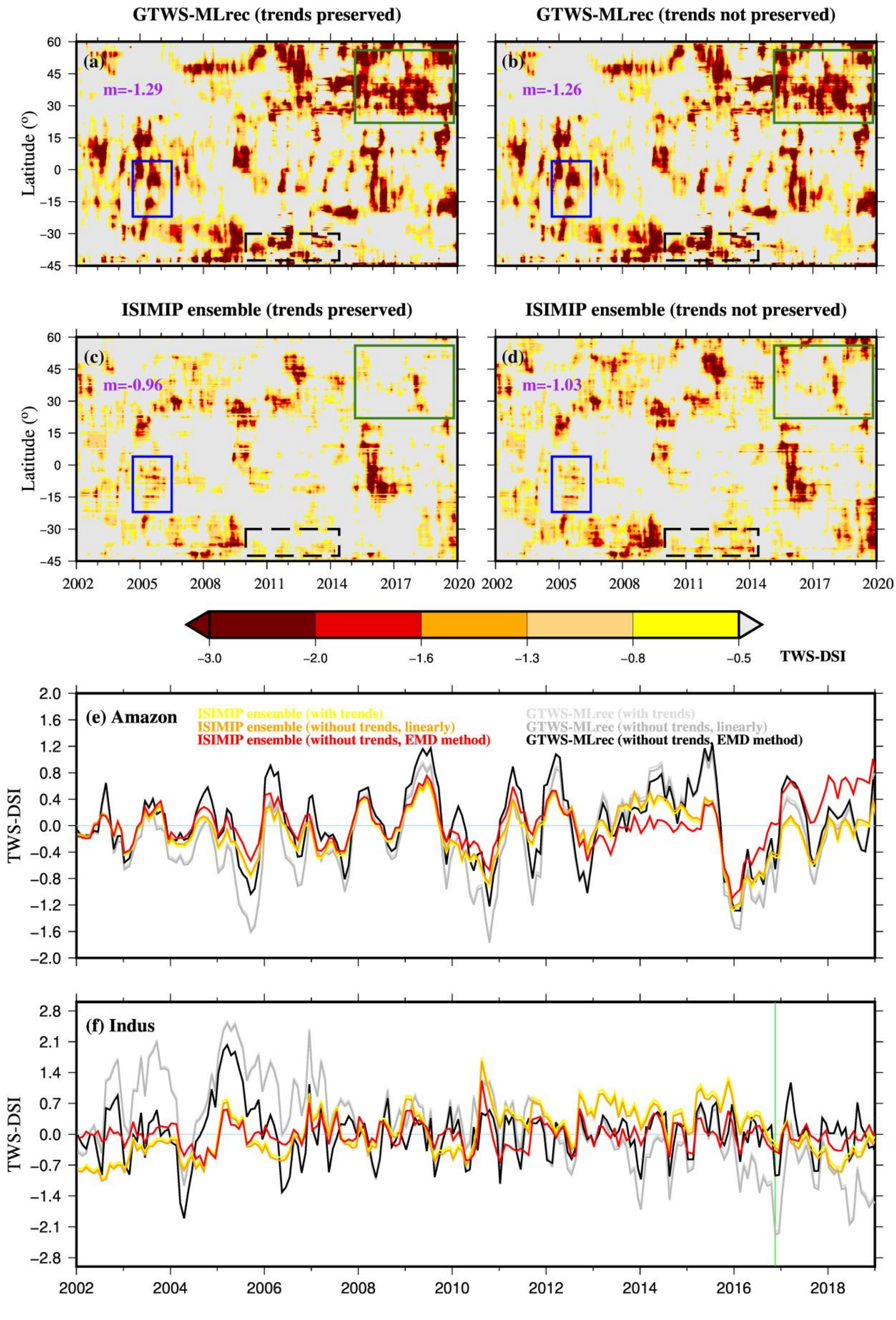
GTWS-MLrec (trends preserved)
GTWS-MLrec (trends not preserved)
(a)
m=-1.29
(b)
m=-1.26
ISIMIP ensemble (trends preserved)
ISIMIP ensemble (trends not preserved)
(c)
m=-0.96
(d)
m=-1.03
Latitude (°)
TWS-DSI
(e) Amazon
ISIMIP ensemble (with trends)
ISIMIP ensemble (without trends, linearly)
ISIMIP ensemble (without trends, EMD method)
GTWS-MLrec (with trends)
GTWS-MLrec (without trends, linearly)
GTWS-MLrec (without trends, EMD method)
(f) Indus

Figure S17. Historical TWS latitudinal droughts from (a) GTWS-MLrec without removing trends in TWSA, (b) GTWS-MLrec after removing trends by linear method, (c) the ensemble median of eight ISIMIP models without removing trends, and (d) the ensemble median of eight ISIMIP models after removing trends by linear method. Here the total record period is 1940-2019 and reference period to remove the mean from TWS is 2004-2009. Selected rectangles highlight major droughts underestimated in the simulations. m values indicate median of TWS-DSI which are below -0.5. (e) comparison of TWS-DSI for Amazon River basin based on ensemble model against GTWS-MLrec TWS for the time period of 1940-2019. (f) same as panel (e) but for Indus River basin.

Basin	GRACE			Simulated								Difference (Months)
	Start date	End date	Duration (Months)	CWatM	H08	HydroPy	JULES-W2	LPJmL5-7-10-fire	MIROC-INTEG-LAND	ORCHIDEE-MICT	WaterGAP2-2e	ENS-GRACE
Mekong	Apr-87	Aug-87	5	4	4	4	4	4	4	4	4	-1
	Nov-94	Jul-95	8	1	3	3	1	2	0	0	1	-7
	May-98	Sep-98	5	0	4	5	7	5	5	6	4	0
Danube	Feb-90	Aug-90	6	17	16	16	17	16	18	14	15	10
	Jun-92	Oct-92	5	7	6	7	9	8	6	5	6	1.5
	Jul-94	Nov-94	5	2	2	3	5	2	4	4	3	-2
Orange	Jan-83	May-83	5	5	6	5	10	6	9	10	4	1
	Feb-86	Sep-86	8	2	3	3	4	6	8	2	1	-5
	Jan-92	Sep-93	21	12	7	13	5	7	15	13	12	-9
RioGrande	Sep-82	Nov-82	3	3	1	4	0	0	0	2	0	-2.5
	Sep-93	Mar-94	7	0	0	0	0	0	0	0	0	-7
	Mar-99	Feb-00	12	5	7	7	4	2	6	7	7	-5.5
Orinoco	May-84	Jul-84	3	0	1	2	3	4	3	2	4	-0.5
	Feb-88	Jul-88	6	2	4	5	4	4	2	3	4	-2
	Sep-97	Feb-98	6	6	7	7	7	8	5	7	7	1
Murray	Jul-82	Apr-83	10	10	9	10	8	10	9	9	9	-1
	Mar-91	Jun-91	4	0	0	1	0	0	0	0	0	-4
	May-97	Jun-98	14	0	3	1	1	3	0	0	1	-13

Figure S18. Observed (reference: GTWS-MLrec) and simulated drought events (TWS-DSI ≤ -0.5) between 1981 and 2000 for selected River basin in each continent. Displayed is each observed drought's start and end date, with the numbers indicating the observed and simulated drought duration in months. Green color shows overestimation while orange color shows underestimation in droughts.

Table S1: Details of Intergovernmental Panel on Climate Change (IPCC) Sixth Assessment Report (AR6) climate zones climate zones

S. No	Acronym	Name	Continent
1	GIC	Greenland/Iceland	POLAR
2	NWN	N.W.North-America	NORTH-AMERICA
3	NEN	N.E.North-America	NORTH-AMERICA
4	WNA	W.North-America	NORTH-AMERICA
5	CNA	C.North-America	NORTH-AMERICA
6	ENA	E.North-America	NORTH-AMERICA
7	NCA	N.Central-America	CENTRAL-AMERICA
8	SCA	S.Central-America	CENTRAL-AMERICA
9	CAR	Caribbean	CENTRAL-AMERICA
10	NWS	N.W.South-America	SOUTH-AMERICA
11	NSA	N.South-America	SOUTH-AMERICA
12	NES	N.E.South-America	SOUTH-AMERICA
13	SAM	South-American-Monsoon	SOUTH-AMERICA
14	SWS	S.W.South-America	SOUTH-AMERICA
15	SES	S.E.South-America	SOUTH-AMERICA
16	SSA	S.South-America	SOUTH-AMERICA
17	NEU	N.Europe	EUROPE
18	WCE	West&Central-Europe	EUROPE
19	EEU	E.Europe	EUROPE
20	MED	Mediterranean	EUROPE-AFRICA
21	SAH	Sahara	AFRICA
22	WAF	Western-Africa	AFRICA
23	CAF	Central-Africa	AFRICA
24	NEAF	N.Eastern-Africa	AFRICA
25	SEAF	S.Eastern-Africa	AFRICA
26	WSAF	W.Southern-Africa	AFRICA
27	ESAF	E.Southern-Africa	AFRICA
28	MDG	Madagascar	AFRICA
29	RAR	Russian-Arctic	ASIA
30	WSB	W.Siberia	ASIA
31	ESB	E.Siberia	ASIA
32	RFE	Russian-Far-East	ASIA
33	WCA	W.C.Asia	ASIA
34	ECA	E.C.Asia	ASIA
35	TIB	Tibetan-Plateau	ASIA
36	EAS	E.Asia	ASIA
37	ARP	Arabian-Peninsula	ASIA
38	SAS	S.Asia	ASIA
39	SEA	S.E.Asia	ASIA

40	NAU	N.Australia	OCEANIA
41	CAU	C.Australia	OCEANIA
42	EAU	E.Australia	OCEANIA
43	SAU	S.Australia	OCEANIA
44	NZ	New-Zealand	OCEANIA

Table S2: Level of human influence on models (Tiwari et al., 2025)

S. No.	Model	Groundwater Withdrawal	Irrigation	Land use change effects	Dams and reservoirs
1	CWatM	Yes	Yes	Used Hyde 3.2 database	Yes
2	H08	Yes	Yes	Irrigation area expansion	Yes
3	HydroPy	Yes	Yes	Chances in crop fraction	No
4	JULES-W2	No	No	ISIMIP3a time varying land use	No
5	LPJmL5-7-10-fire	No	Yes	ISIMIP3a time varying land use	Yes
6	MIROC-INTEG-LAND	No	Yes	ISIMIP3a time varying land use	Yes
7	ORCHIDEE-MICT	No	No	ISIMIP3a time varying land use	No
8	WaterGAP2-2e	Yes	Yes	Only static land use map is used but irrigation area is changing over time	Yes

Table S3: Details of models with TWS and its components (Tiwari et al., 2025)

S. No.	Model	TWS components utilized in the model simulations	TWS components outputs							
1	**cwatm**	groundwater, soil, lakes and reservoirs, channels, snow, canopy	canopy stor	groundwstor	lakestor	reservoir stor	riverstor	soilmoist	swe	
2	**h08**	groundwater, soil moisture, river storage, large and medium reservoirs, and snow		groundwstor		reservoir stor	riverstor	soilmoist	swe	
3	**hydropy**	snow, canopy, soil, rivers, lakes, groundwater	canopy stor	groundwstor	lakestor		riverstor	soilmoist	swe	
4	**jules-w2**		canopy stor				riverstor	soilmoist	swe	
5	**LPJmL5-7-10-fire**	soilmoist + lakestor + riverstor + reservoirstor + swe + litter storage + short-term irrigation storage			lakestor	reservoir stor	riverstor	soilmoist	swe	
6	**miroc-integ-land**	soilmoist, canopystor, swe, riverstor, reservoirstor'	canopy stor			reervoir stor	riverstor	soilmoist	swe	
7	**Orchidee-mict**							soilmoist	swe	
8	**watergap 2-2e**	canopystor + riverstor + swe + soilmoist + groundwstor + lakestor + wetlandstor + reservoirstor	canopy stor	groundwstor	lakestor	reservoir stor	riverstor	soilmoist	swe	wetland stor

References

Kumar, A., Gosling, S. N., Johnson, M. F., Jones, M. D., Zaherpour, J., Kumar, R., et al. (2022). Multi-model evaluation of catchment- and global-scale hydrological model simulations of drought characteristics across eight large river catchments. Advances in Water Resources, 165. https://doi.org/10.1016/j.advwatres.2022.104212

Tiwari, A. D., Pokhrel, Y., Boulange, J., Burek, P., Guillaumot, L., Gosling, S. N., et al. (2025). Similarities and divergent patterns in hydrologic fluxes and storages simulated by global water models. *Nature Water*. https://doi.org/10.1038/s44221-025-00435-6